JOURNAL OF GEOPHYSICAL RESEARCH, VOL. 102, NO. A4, PAGES 7485–7492, APRIL 1, 1997

A plasma temperature anomaly in the equatorial topside ionosphere

N. Balan,[1,2] K.-I. Oyama,[3] G. J. Bailey,[4] S. Fukao,[1] S. Watanabe,[5] and M. A. Abdu[6]

Abstract. A study of the thermal structure of the low-latitude (30°N to 30°S) ionosphere under equinoctial conditions at low, medium, and high solar activity has been carried out using the Sheffield University plasmasphere-ionosphere model (SUPIM) and Hinotori satellite observations. The study reveals the existence of an anomaly in the plasma (electron and ion) temperature in the topside ionosphere during the evening-midnight period. The anomaly, called the equatorial plasma temperature anomaly (EPTA), is characterized by a trough around the magnetic equator with crests on either side. The trough develops before the crests. The model results show that the anomaly occurs between 1900 and 0100 LT at altitudes between 450 and 1250 km; the strongest anomaly occurs around 2130 LT at 950 km altitude during high solar activity. The temperature trough of the anomaly arises from the adiabatic expansion of the plasma and an increase in plasma density caused by the prereversal strengthening of the upward vertical $\mathbf{E} \times \mathbf{B}$ drift. The temperature crests arise from the combined effect of the reverse plasma fountain and nighttime plasma cooling. The electron temperature measured by the Hinotori satellite near 600 km altitude during medium and high solar activity periods shows the existence of the EPTA with characteristics in close agreement with those obtained by the model. The model also reproduces the occurrence of a daytime temperature bulge in the electron temperature in the bottomside ionosphere; the ion temperature shows no bulge.

1. Introduction

The horizontal orientation of the geomagnetic field at the geomagnetic equator is known to be the basic reason for many unique features observed in the low-latitude ionosphere, (e.g., the equatorial electrojet, equatorial plasma fountain, equatorial ionization anomaly, plasma bubbles, and spread F). Review articles of the low-latitude ionosphere have been presented by *Rajaram* [1977], *Moffett* [1979], *Anderson* [1981], *Walker* [1981], *Ossakow* [1981], *Reddy* [1981], *Kelley* [1985], *Sastri* [1990], *Abdu et al.* [1991], *Stening* [1992], *Bailey et al.* [1996], and *Abdu* [1997]. The low-latitude thermosphere is also known to exhibit unique features in density, temperature, and wind speed; the density and temperature exhibit small anomalies similar to the equatorial ionization anomaly, and the zonal wind speed at the anomaly trough (dip equator) is 50–100 m s^{-1} faster than the wind speed near the anomaly crests [*Hedin and Mayr*, 1973; *Raghavarao et al.*, 1991]. Recently, through modeling studies and observations it has been shown that the horizontal orientation of the geomagnetic field at the geomagnetic equator also leads to the formation of an additional layer, the F_3 layer, near the geomagnetic equator [*Balan and Bailey*, 1995; *Balan et al.*, 1997; *Bailey et al.*, 1997]. The aim of the present study is to investigate the existence of a recently observed feature of the low-latitude ionosphere that also arises from the horizontal orientation of the geomagnetic field at the geomagnetic equator. This feature is called the equatorial plasma temperature anomaly (EPTA) and is seen in the low-latitude plasma temperature variations modeled by the Sheffield University plasmasphere-ionosphere model and the Hinotori satellite observations.

Plasma temperature variations in the ionosphere have been studied extensively through ground-based and in situ observations and through theoretical calculations. Excellent reviews of the observations and theory have been presented by *Sayers* [1970], *Bauer and Nagy* [1975], *Schunk and Nagy* [1978], *Farley* [1991], and *Oyama and Schlegel* [1988]. *Brace and Theis* [1981] and *Kohnlein* [1986] have presented empirical models of electron temperature in the ionosphere and lower plasmasphere. Theoretical models have also been used to study the temperature variations in the ionosphere and plasmasphere [*Richards and Torr*, 1986; *Khazanov et al.*, 1993; *Watanabe et al.*, 1995]. Recently, the Sheffield University plasmasphere-ionosphere model (SUPIM) has been used to investigate the electron temperature in the ionosphere and plasmasphere measured by the Hinotori and Exos D satellites [*Su et al.*, 1995; *Oyama et al.*, 1996; *Balan et al.*, 1996a, b].

Oyama et al., [1997] have reported the existence of an electron temperature anomaly in the low-latitude ionosphere near 600 km altitude during evening hours at the equinoxes under high levels of solar activity ($F_{10.7} > 250$). They have also

[1]Radio Atmospheric Science Center, Kyoto University, Uji, Kyoto, Japan.
[2]On leave from Department of Physics, University of Kerala, Trivandrum, India.
[3]Institute of Space and Astronautical Science, Sagamihara, Kanagawa, Japan.
[4]School of Mathematics and Statistics, Applied Mathematics Section, University of Sheffield, Sheffield, England.
[5]Department of Astronomy and Geophysics, Tohoku University, Aramaki, Aoba, Sendai, Japan.
[6]Instituto Nacional de Pesquisas Espaciais, São José dos Campos, São Paulo, Brazil.

Paper number 97JA00039.
0148-0227/97/97JA-00039$09.00

found an association between the electron temperature anomaly and the equatorial ionization anomaly. Presented in this paper are results of an investigation of the plasma temperature variations in the low-latitude ionosphere at equinox under conditions of high, medium, and low solar activity. It will be shown that while the ionospheric peak and bottomside ionosphere are almost isothermal in latitude during both day and night, an anomaly in the plasma temperature (EPTA) exists over a large altitude range in the topside ionosphere during the evening-midnight period at all levels of solar activity. The anomaly, which exists in both the electron and ion temperatures, arises from a combined manifestation of the vertical **E** × **B** drift velocity and nighttime plasma cooling.

2. Model Calculations and Data

As mentioned above, the study is carried out using values modeled by SUPIM [*Bailey and Sellek*, 1990; *Bailey et al.*, 1993; *Bailey and Balan*, 1996] and observations made by the Hinotori satellite [*Oyama et al.*, 1988]. In SUPIM, coupled time-dependent equations of continuity, momentum, and energy balance for the O^+, H^+, He^+, N_2^+, O_2^+, and NO^+ ions and electrons are solved along closed-dipole magnetic field lines between base altitudes of about 130 km in conjugate hemispheres to give values for the concentrations, field-aligned fluxes, and temperatures of the ions and electrons at a discrete set of points along the field lines. For the present study, the model equations are solved along 114 eccentric-dipole magnetic field lines distributed with apex altitude between 150 and 5000 km and with the number of points along the field lines increasing with apex altitude from 201 to 301; this gives a reasonable 24-hour distribution of model data between 200 and 2000 km altitude and ±30° magnetic latitude. Further details are provided by *Balan and Bailey* [1995] and *Bailey and Balan* [1996].

The model data are obtained for magnetically quiet (Ap = 4) equinoctial conditions (day 264) at high ($F_{10.7}$ = 178, $F_{10.7A}$ = 202), medium ($F_{10.7}$ = 145, $F_{10.7A}$ = 164), and low ($F_{10.7}$ = 85, $F_{10.7A}$ = 72) solar activity levels at longitude 77°W. This longitude approximates the longitudes of Jicamarca and Arecibo, where accurate measurements of the perpendicular **E** × **B** plasma drift velocities (which are important for low-latitude studies) are made. The drift velocities are known to have altitude and latitude variations. The altitude variation is accounted for in the model calculations by using the drift velocities (see Figure 1) measured at Jicamarca [*Fejer et al.*, 1991] for magnetic field lines with apex altitude less than 450 km and those measured at Arecibo [*Fejer*, 1993], scaled to the magnetic equator, for field lines with apex altitude greater than 2000 km; a linear interpolation is used for the field lines at intermediate apex altitudes. Drift velocities at Arecibo are not available for medium solar activity and so are deduced from those available at low and high levels of solar activity (Figure 1). The importance of including an altitude variation in the vertical **E** × **B** drift velocity model has been demonstrated by *Su et al.* [1995]. The drift velocity varies along the magnetic field lines in accordance with the field line geometry [*Bailey et al.*, 1993]. A characteristic feature of the equatorial drift velocity is the evening prereversal upward strengthening followed by a large downward drift (see Figure 1). This feature of the drift has been observed at all longitudes [*Namboothiri et al.*, 1989; *Hari and Krishna Murthy*, 1995; *Batista et al.*, 1996] and leads to the formation of plasma bubbles and spread F. This

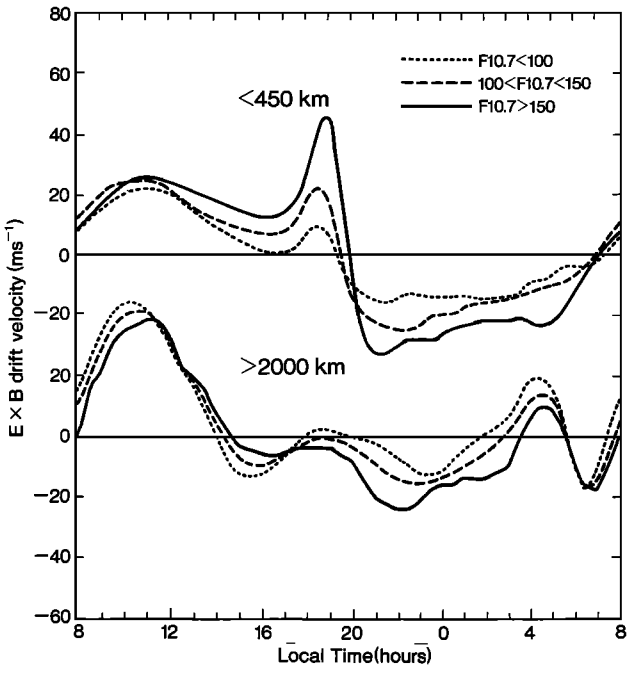

Figure 1. Local time variations of the equatorial vertical **E** × **B** drift velocity (upward is positive) used in the model calculations for the apex altitudes noted. A linear interpolation is used for the intermediate apex altitudes.

feature also leads to the formation of the equatorial plasma temperature anomaly (EPTA) described in the present paper. The zonal **E** × **B** plasma drift is neglected [*Anderson*, 1981]. The neutral wind velocity in the magnetic meridian, which also varies with altitude and latitude, is determined from the meridional and zonal wind velocities given by the thermospheric Hedin wind model 1990 (HWM90) [*Hedin et al.*, 1991]. The concentrations and temperatures of the neutral gases are taken from the mass spectrometer incoherent scatter 1986 (MSIS86) thermospheric model [*Hedin*, 1987], and the solar EUV fluxes are taken from the EUV94 solar EUV flux model (a revised version of the EUV91 solar EUV flux model [*Tobiska*, 1991]). The EUV94 model is known to produce a higher integrated solar EUV flux for a given $F_{10.7}$ than other models like the EUVAC model [*Richards et al.*, 1994]. However, the difference in EUV flux does not affect the occurrence and development of EPTA because EPTA occurs after sunset and for all levels of solar activity (see section 3.1).

The photoelectron heating rates are calculated by the model developed by *Richards and Torr* [1986, 1988]. This model uses the two-stream approximation method of *Banks and Nagy* [1970] and includes interhemispheric transport of photoelectrons. Photoelectrons escaping from one ionosphere and traveling to the conjugate ionosphere through the plasmasphere heat the thermal electrons through Coulomb collisions, magnetic trapping due to pitch angle diffusion, and backscattering from the conjugate ionosphere before being thermalized. In the model, backscattering is included self-consistently, and pitch angle diffusion is taken care of by assuming that a fraction of the photoelectrons is trapped and that all the energy of the trapped flux is deposited in the plasmasphere. A photoelectron trapping factor of 50%, consistent with that used by *Newberry et al.* [1989], *Khazanov and Liemohn* [1995], and *Balan et al.* [1996b], is used in the present study. The photo-

electron trapping (50%) has the effect of keeping the nighttime electron temperature in the low-latitude topside ionosphere high by about 150 K [*Balan et al.*, 1996b]. However, the trapping, as determined from model calculations carried out with and without photoelectron trapping, has no significant effect on the occurrence and development of EPTA because this anomaly occurs only after sunset. Photoelectrons from the conjugate hemisphere also have no significant effect on EPTA; the EPTA occurs mainly in equinox (see section 3.2) when sunset is almost simultaneous in the two hemispheres.

The electron temperature data used in the present study were obtained from the observations made during the years 1981 and 1982 by the electron temperature probe on board the Hinotori satellite [*Oyama et al.*, 1988; *Watanabe and Oyama*, 1996]. The Hinotori satellite had a circular orbit at an altitude near 600 km, and the inclination was 31°. The data obtained during the equinoctial months of March and April (1981 and 1982) and September and October (1981) have been used in the present study with no separation for longitude. The $F_{10.7}$ solar activity index varied from 130 to 303 during these periods.

3. Results and Discussion

3.1. Model Results

The model results shown in Figures 2–4 are for high solar activity, and those shown in Figure 5 are for medium and low solar activities. Figure 2a shows the latitude variation of the modeled electron temperature at several altitudes at 1830 and 2130 LT. These local times are close to the maximum upward and maximum downward equatorial vertical **E** × **B** drift velocity, respectively. As Figure 2a shows, the well-known daytime electron temperature bulge [*Bilitza*, 1987; *Farley*, 1991] exists at 1830 LT at altitudes below 350 km around the equator; at later times (2130 LT) the peak and bottomside ionospheres become almost isothermal in latitude. However, an anomaly in the plasma temperature (EPTA) exists in the topside ionosphere during the evening-midnight period. The anomaly is characterized by a temperature trough around the magnetic equator with crests on either side. The trough develops before the reversal of the **E** × **B** drift (1945 LT) and the crests develop shortly afterward. Figure 2b is similar to Figure 2a but has been obtained from model calculations that exclude the **E** × **B** drift. A comparison of Figures 2a and 2b clearly demonstrates that the EPTA is caused by the vertical **E** × **B** drift velocity.

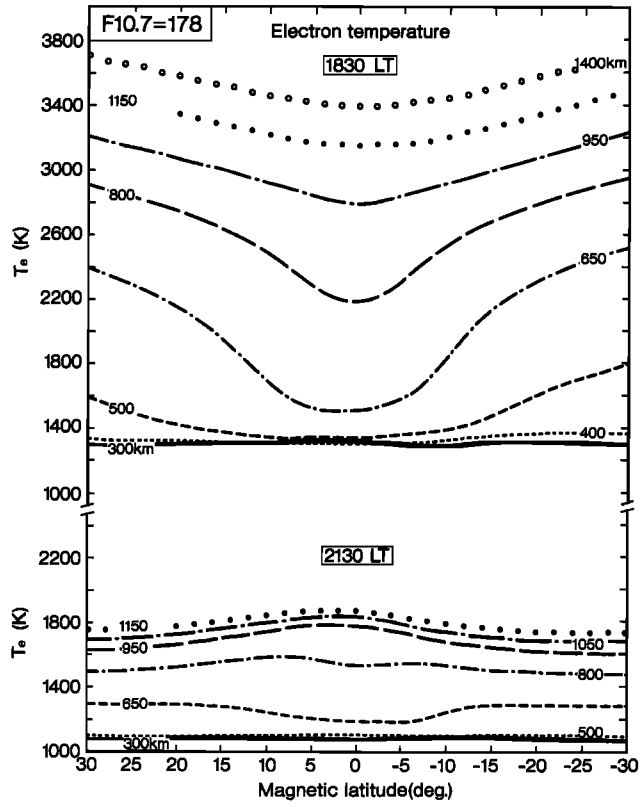

Figure 2b. Same as Figure 2a, but obtained from model calculations with zero **E** × **B** drift velocity.

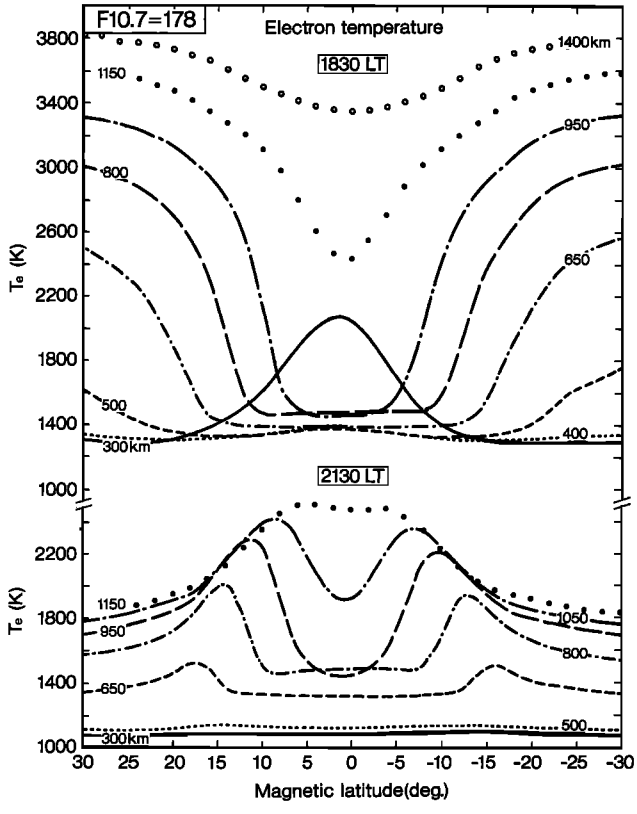

Figure 2a. Latitude variations of modeled electron temperature for various altitudes at 1830 and 2130 LT at high solar activity; positive magnetic latitude is northward.

A further comparison of Figures 2a and 2b reveals that the temperature trough of the EPTA is a composite of two effects, a minor effect and a major effect. The minor effect occurs in the absence of the **E** × **B** drift and contributes to the temperature trough at altitudes near 700 km (Figure 2b); this effect could arise from the latitude variation of the electron density in the absence of the **E** × **B**, which has a maximum around the equator. The major effect, which can be seen by differencing corresponding curves in Figures 2a and 2b, is important between about 500 and 1400 km altitude and is strongest (about 1500 K) at around 950 km altitude. The major effect is caused by the prereversal strengthening of the equatorial upward **E** × **B** drift. As the plasma drifts from lower to higher field lines, it undergoes adiabatic expansion in the topside ionosphere, while at the same time, the plasma density increases above the nondrift value, especially during the prereversal period when the upward **E** × **B** force increases rapidly. Both the adiabatic

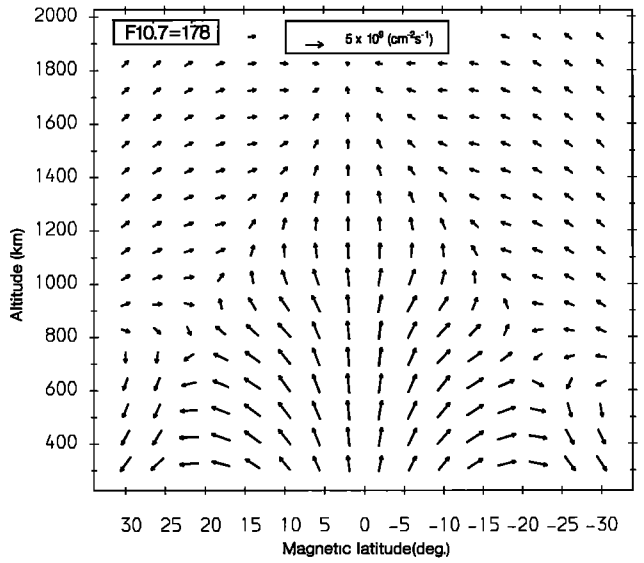

Figure 2c. Vector plasma fluxes at 1830 LT at high solar activity. The fluxes are plotted in log scale, and the minimum vector length (zero length) corresponds to plasma fluxes less than 10^6 cm^{-2} s^{-1}; positive magnetic latitude is northward.

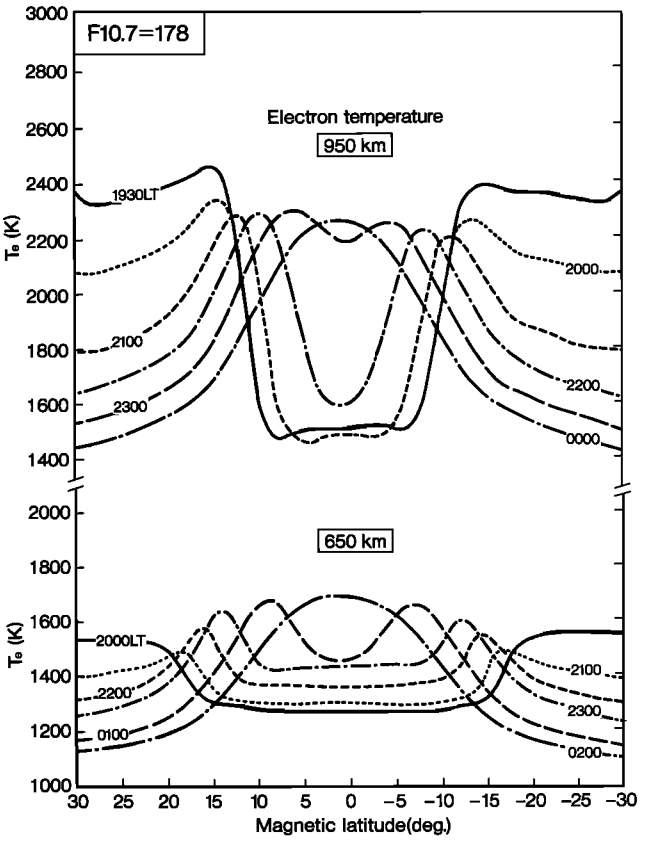

Figure 3a. Latitude variations of modeled electron temperature at altitudes of 950 and 650 km for various local times at high solar activity; positive magnetic latitude is northward.

expansion and increase in plasma density cause the plasma temperature to decrease (i.e., to create a trough in the plasma temperature). Also, the plasma that has drifted upward from the ionospheric peak and bottomside ionosphere is comparatively cold; this may make a contribution to the temperature trough. The vector plot of the plasma fountain at 1830 LT (Figure 2c) shows that the altitude-latitude coverage of the temperature trough (Figure 2a) corresponds to that of the plasma fountain. At and below the ionospheric peak where plasma drifts from lower to higher density, the **E** × **B** drift has little effect on plasma temperature.

The electron and ion temperatures, as expected for low latitudes at night, are found to be almost equal and to exhibit almost identical EPTAs. This is illustrated in Figures 3a and 3b, which show almost identical local time evolutions of the EPTA for the electrons and ions at 650 km altitude. Figure 3a also contains the local time evolution of the EPTA at an altitude of 950 km for the electrons. As Figure 3a shows, the temperature crests of the EPTA appear and disappear earlier at higher altitudes and later at lower altitudes; the crest to trough temperature difference reaches a maximum at around 950 km altitude, where the deepest temperature trough forms (see Figure 2a). At 950 km altitude the crests appear before 2000 LT and disappear by midnight; the maximum crest to trough difference is about 700 K at around 2130 LT. At the lower altitude of 650 km the crests appear after 2030 LT and disappear after midnight; the maximum crest to trough difference is about 200 K at around 2200 LT. At all altitudes when the crests disappear, the latitude variation of temperature shows a maximum at the magnetic equator.

The local time evolution of the EPTA can be explained as follows. After sunset the plasma temperature is expected to decrease at all altitudes and latitudes because of nighttime plasma cooling. However, in the topside ionosphere (see Figure 3a) the temperature decreases only at latitudes outside the temperature trough where the heat capacity is low. Inside the temperature trough where the heat capacity is high because of the high plasma density caused by the prereversal strengthening of the upward **E** × **B** drift and where the plasma temperature has fallen close to the neutral temperature, the temperature remains steady initially and then increases. Consequently, temperature crests appear on either side of the temperature trough before the trough disappears. The crests appear earlier at higher altitudes; at these altitudes the plasma cools faster because of the lower heat capacity caused by the lower plasma content. The temperature increases inside the trough are caused by the reverse plasma fountain, which brings

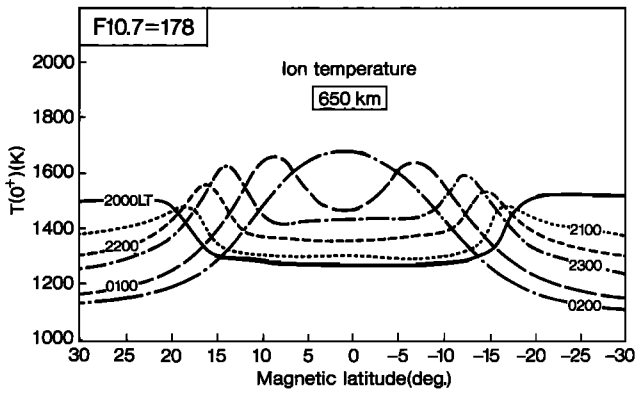

Figure 3b. Latitude variations of modeled ion temperature at 650 km altitude for various local times at high solar activity; positive magnetic latitude is northward.

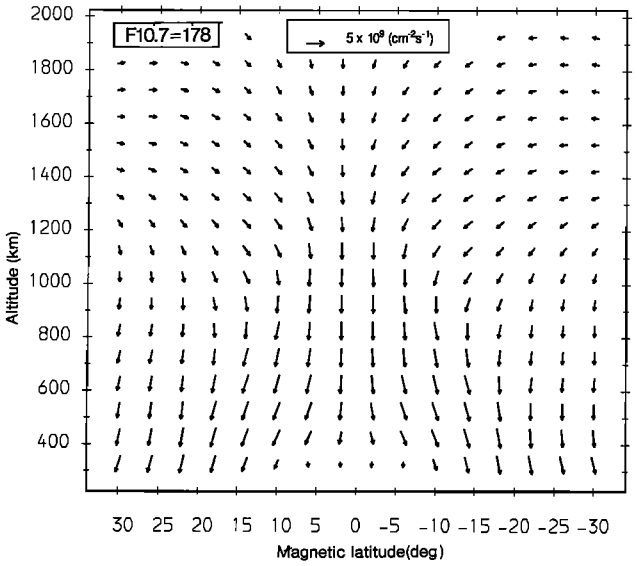

Figure 3c. Vector plasma fluxes at 2100 LT at high solar activity. The fluxes are plotted in log scale, and the minimum vector length (zero length) corresponds to plasma fluxes less than 10^6 cm^{-2} s^{-1}; positive magnetic latitude is northward.

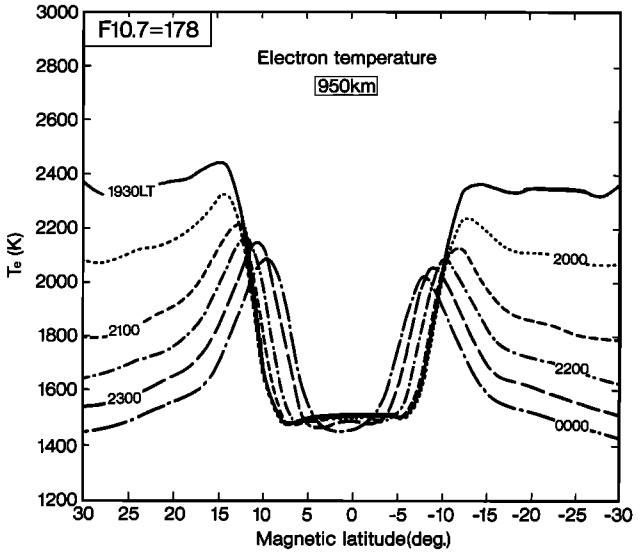

Figure 4a. Same as Figure 3a (950 km), but obtained from model calculations with zero **E** × **B** drift velocity during 2000–2400 LT.

hot plasma from higher altitudes and latitudes to lower altitudes and latitudes and also causes adiabatic compression of plasma around the equator. A vector plot of the reverse plasma fountain at 2100 LT is shown in Figure 3c. The reverse plasma fountain raises the temperature faster at higher altitudes because of lower heat capacity and, consequently, causes earlier disappearance of the EPTA at these altitudes (see Figure 3a).

As discussed above, the raising of the temperature inside the trough and the subsequent disappearance of the EPTA is caused by the large postreversal downward **E** × **B** drift velocity (see Figure 1) and the associated reverse plasma fountain. Then, at times when the downward **E** × **B** drift velocity is small, the temperature inside the trough, which has fallen close to the neutral temperature, may remain steady. This feature is found to be true in the model values illustrated in Figure 4a. This figure is similar to the 950-km section of Figure 3a and has been constructed from model calculations with zero drift velocity during the period 2000–2400 LT. When the nighttime downward **E** × **B** drift is absent, the temperature inside the trough remains almost steady; the movement of the temperature crests to lower latitudes with time, similar to the movement of the ionization anomaly crests, is also clear in Figure 4a.

Figure 4b shows altitude profiles of the electron temperature at the magnetic equator at different local times and of the ion temperature at 1200 LT. The electron and ion temperatures are found to have the same behaviors at all altitudes except in the bottomside ionosphere during daytime. In the bottomside ionosphere, as shown by incoherent scatter observations [*Farley*, 1991], the electrons exhibit a daytime temperature bulge; the ions do not exhibit such a bulge. In the topside ionosphere both the electrons and ions exhibit a small temperature minimum at an altitude which corresponds to the F_3 layer [*Balan et al.*, 1997; *Bailey et al.*, 1997]. This minimum, which is present at around 650 km altitude at noon, moves upward to about 1000 km altitude by evening and then moves downward and disappears by midnight. The feature shown in Figure 4b, which is of particular interest in the present study, is the presence of a nighttime temperature maximum in the topside ionosphere which descends in altitude during the night. Such a temperature maximum, which arises from adiabatic plasma compression around the magnetic equator, has been observed in the nighttime electron temperature profiles obtained from Exos D satellite measurements [*Balan et al.*, 1996a, b].

The analysis of the model data obtained for the three levels of solar activity shows that the EPTA occurs at all levels of solar activity during equinoctial periods. The EPTA becomes strong, extends to higher altitudes, and lasts longer with increasing solar activity; the EPTA is found to last from less than 2 hours (1900–2100 LT) at solar minimum to more than 5 hours (1930–0100 LT) at solar maximum. Figure 5 shows the EPTA obtained for medium ($F_{10.7}$ = 145) and low ($F_{10.7}$ = 85) solar activities at 2100 and 1930 LT, respectively. A com-

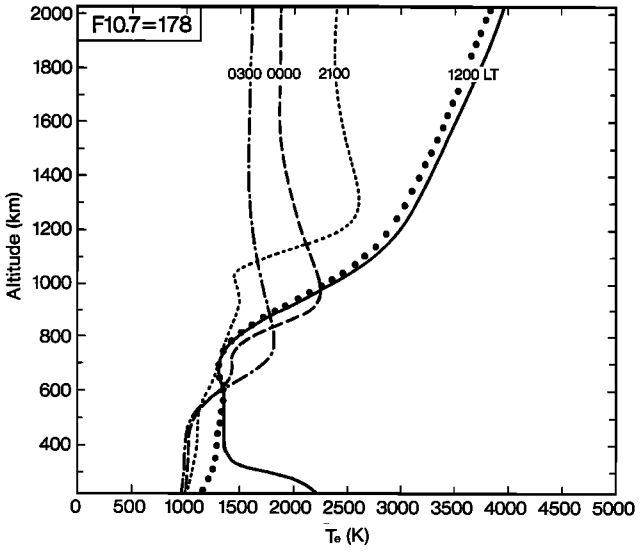

Figure 4b. Altitude profiles of modeled electron temperature at various local times at high solar activity. The large dots show the ion temperature profile at 1200 LT.

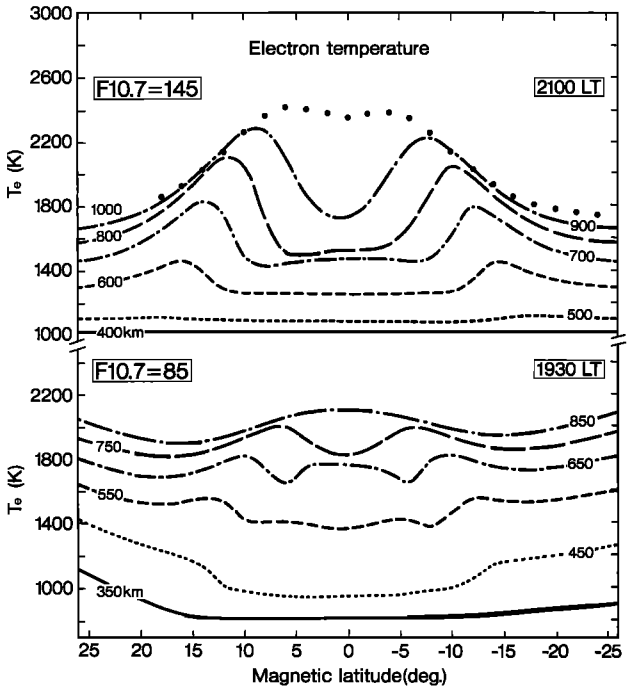

Figure 5. Latitude variations of modeled electron temperature at various altitudes at (top) 2100 LT at medium solar activity and at (bottom) 1930 LT at low solar activity; positive magnetic latitude is northward.

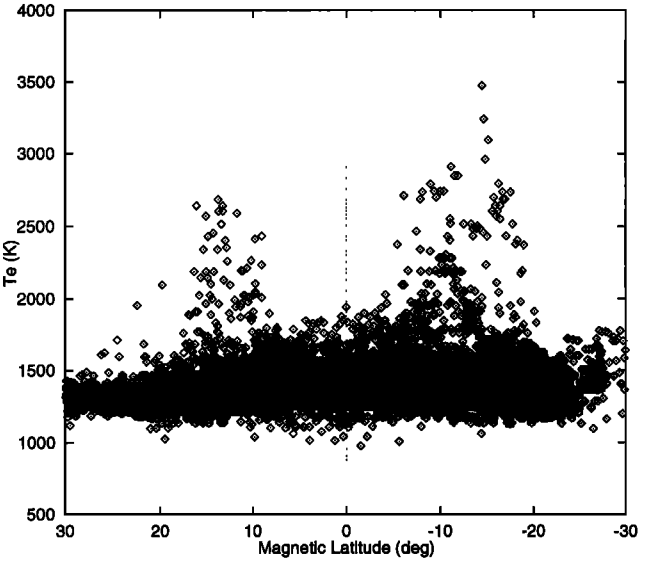

Figure 6a. Latitude variation of measured electron temperature near 600 km altitude; the data are for the equinoctial months March and April (1981 and 1982) and September and October (1981) at 30-min intervals during the period 2000–2300 LT; positive magnetic latitude is northward.

parison of Figure 2a and Figure 5 shows that as the solar activity increases, the strongest EPTA occurs later in local time and at higher altitudes. Figure 5 also indicates that the altitude and local time of occurrence of EPTAs can have large variability even for a particular solar activity level. This is due to the large day-to-day variability of the prereversal and postreversal **E** × **B** drift velocities, which produce and control the evolution of the EPTA.

3.2. Experimental Results

The model results presented above suggest that the EPTA should be detectable at 600 km altitude and therefore by the electron temperature probe on board the Hinotori satellite. In addition, at all levels of solar activity an EPTA should be expected to occur frequently during equinox at times when the equatorial upward **E** × **B** drift velocity undergoes prereversal strengthening, the primary reason for an EPTA, and the neutral wind is almost symmetric about the magnetic equator. As expected, the analysis of the electron temperature data collected by the Hinotori satellite during the 17 months of medium and high solar activity, February 1981 to May 1982, has shown that EPTAs occur more frequently in the equinoctial months and less frequently in the solstice months. Figure 6a, which shows the data for the equinoctial months at 30-min time intervals during 2000–2300 LT, shows the trough and crests of an EPTA. The scatter in the data mainly reflects the temperature variation during 2000–2300 LT and the effect of the day-to-day variability of the prereversal and postreversal **E** × **B** drift velocities. The scatter also includes the effects of longitude and solar activity variations.

To study the local time evolution of the observed EPTA, the data collected between 1745 and 0615 LT have been grouped into time intervals of 30 min, and mean latitude variations have been obtained for each interval. Figure 6b shows the latitude variations at selected local times. In agreement with the model results, only the temperature trough of the EPTA exists before 1900 LT. The temperature crests commence their formation after 1900 LT; the crests are strong at around 2100 LT and have maximum crest to trough differences of about 200 K. The EPTA disappears by midnight. After the disappearance of the EPTA the temperature around the magnetic equator becomes a maximum, although the maximum is small when compared to

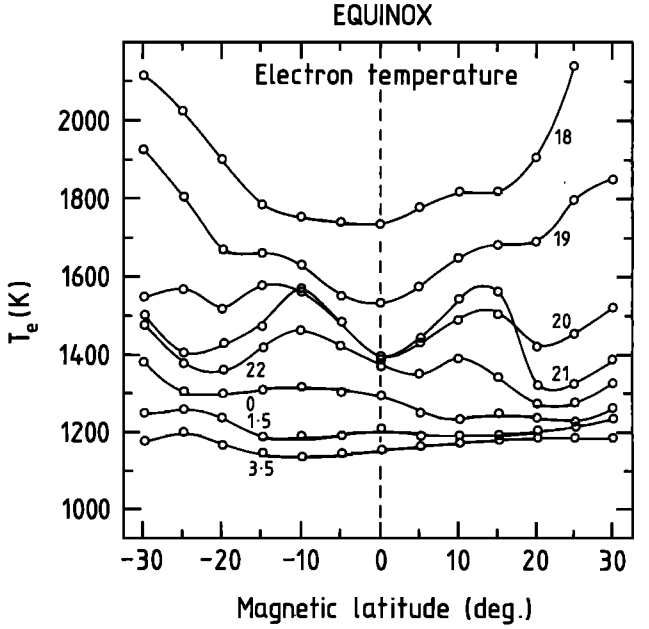

Figure 6b. Latitude variation of 30-min mean measured electron temperature for 600 km altitude at various local times; positive magnetic latitude is northward.

that obtained from the model; a strong nighttime maximum has been observed around the equator at altitudes around 1000 km [*Balan et al.*, 1997, 1996]. Figure 6b also shows that the temperature inside the temperature trough increases with local time only during the period 2000–2100 LT. This is in partial agreement with the modeled EPTAs obtained without downward **E** × **B** drift (see Figure 4a) and with downward **E** × **B** drift (see Figure 3a). It appears therefore that the mean downward **E** × **B** drift velocity for the 6 months of observation of the electron temperature data, when $F_{10.7}$ varied from 130 to 303, could be smaller than that used in the model calculations.

There are other significant differences in the modeled and observed EPTAs, particularly in the time of occurrence of the temperature crests, the time of maximum crest to trough temperature difference, and the time of disappearance of EPTA. These times are up to an hour earlier in the observed EPTA than in the modeled EPTA. The differences are mainly due to the fact that the observed EPTA shows its mean behavior during a 6-month period while the modeled EPTA corresponds to a particular day. As explained above, the EPTA is produced and controlled by the prereversal and postreversal vertical **E** × **B** drift velocity at the magnetic equator and nighttime plasma cooling. The drift velocity has large day-to-day, longitude, and altitude variations in magnitude and time of reversal. These day-to-day variations in the drift velocity and in the nighttime plasma cooling, which are not taken care of in the model calculations, could be the main reason for the differences in the observed and modeled EPTA. Also, the heat conduction across the field lines [*Moffett et al.*, 1993], which is not taken care of in the model, could also cause differences in the observed and modeled temperatures.

The Hinotori data for solstice months (not shown) show large temperature depressions around the magnetic equator during the evening-midnight period, with no clear temperature crests, and the temperature minimum occurs on the summer side of the magnetic equator. This is consistent with the OGO 6 satellite observations, which show large electron and ion temperature depressions around the magnetic equator at altitudes above 500 km on solstice nights [*Hanson et al.*, 1973]. The temperature depressions have been attributed to the expansion cooling of the plasma around the equator because of interhemispheric transport caused by the highly asymmetric neutral wind, which flows from the summer to the winter hemisphere [*Rishbeth et al.*, 1977]. The EPTA studied in the present paper could exhibit its effect in optical emissions from atomic and molecular recombinations. The authors are not aware if such optical effects have been detected.

4. Summary

The thermal structure of the low-latitude (30°N to 30°S) ionosphere under equinoctial conditions at low, medium, and high levels of solar activity has been investigated by using the Sheffield University plasmasphere-ionosphere model (SUPIM) and measurements made by the Hinotori satellite. It has been found that while the ionosphere near and below the F_2 peak is almost isothermal in latitude during both day and night, an anomaly occurs in the plasma (electron and ion) temperature in the topside ionosphere during the evening-midnight period. The anomaly is called the equatorial plasma temperature anomaly (EPTA) and is characterized by a trough in the plasma (electron and ion) temperature around the magnetic equator with crests on either side; the trough develops first and the crests later. The temperature trough of the anomaly arises from the adiabatic expansion of the plasma and increase in plasma density caused by the prereversal strengthening of the upward vertical **E** × **B** drift. The temperature crests arise from the combined effect of the reverse plasma fountain and nighttime plasma cooling. The cooling causes the temperature to decrease with time at latitudes outside the temperature trough. Inside the trough where the heat capacity is high and the temperature has fallen close to the neutral temperature, the plasma temperature remains steady at the beginning and then increases. Consequently, temperature crests occur on either side of the temperature trough before the trough disappears. The increase in temperature inside the temperature trough is caused by the reverse plasma fountain which brings hot plasma from higher altitudes and latitudes to lower altitudes and latitudes and also causes compression heating of plasma around the equator. The model results also reproduce the occurrence of daytime temperature bulge in the bottomside in electron temperature, which is absent in ion temperature.

The model results show that an EPTA can occur between 1900 and 0100 LT and between 450 and 1250 km altitude; the time of duration can range from less than 2 hours (1900–2100 LT) at solar minimum to more than 5 hours (1930–0100 LT) at solar maximum, and the altitude range can vary from 450–750 km at solar minimum to 550–1250 km at solar maximum. At each level of solar activity the anomaly, which appears and disappears earlier at higher altitudes, becomes strong at intermediate altitudes. During high solar activity the anomaly is found to have a maximum crest to trough temperature difference of about 700 K at 950 km altitude and 200 K near 600 km altitude. The electron temperature measured by the Hinotori satellite near 600 km altitude during medium-high solar activity periods shows the existence of EPTAs with characteristics in close agreement with those obtained from the model. Also, as expected from the effect of the reverse plasma fountain, the model and observed data show that the temperature around the magnetic equator becomes a maximum at the time when the EPTA disappears. There are some significant differences in the modeled and observed EPTAs, which could be caused by the day-to-day variations of the prereversal and postreversal vertical **E** × **B** drift velocity at the equator and nighttime plasma cooling.

Acknowledgments. The authors would like to express their sincere thanks to P. G. Richards of the Computer Science Department and the Center for Space Plasma and Aeronomic Research, University of Alabama in Huntsville for providing the photoelectron heating code for inclusion into SUPIM. The authors would also like to express their sincere thanks to all members of the Hinotori project. N. Balan would like to thank the Institute of Space and Astronautical Science (Japan) and the Radio Atmospheric Science Center (RASC) of Kyoto University (Japan) for providing visiting fellowships.

The Editor thanks R. Link for his assistance in evaluating this paper.

References

Abdu, M. A., Major phenomena of the equatorial ionosphere-thermosphere system under disturbed conditions, *J. Atmos. Terr. Phys.*, in press, 1997.

Abdu, M. A., J. H. A. Sobral, E. R. de Paula, and I. S. Batista, Magnetospheric disturbance effects on the equatorial ionization anomaly (EIA): An overview, *J. Atmos. Terr. Phys.*, *53*, 757, 1991.

Anderson, D. N., Modeling the ambient, low latitude *F*-region ionosphere—A review, *J. Atmos. Terr. Phys.*, *43*, 753, 1981.

Bailey, G. J., and N. Balan, A low-latitude ionosphere-plasmasphere model, in *STEP Handbook*, edited by R. W. Schunk, pp. 173–206, Utah State Univ. Press, Logan, 1996.

Bailey, G. J., and R. Sellek, A mathematical model of the Earth's plasmasphere and its application in a study of He^+ at $L = 3$, *Ann. Geophys.*, *8*, 171, 1990.

Bailey, G. J., R. Sellek, and Y. Rippeth, A modeling study of the equatorial topside ionosphere, *Ann. Geophys.*, *11*, 263, 1993.

Bailey, G. J., N. Balan, and Y. Z. Su, The Sheffield University plasmasphere-ionosphere model—A review, *J. Atmos. Terr. Phys.*, in press, 1997.

Balan, N., and G. J. Bailey, Equatorial plasma fountain and its effects: Possibility of an additional layer, *J. Geophys. Res.*, *100*, 21,421, 1995.

Balan, N., K.-I. Oyama, G. J. Bailey, and T. Abe, Plasmasphere electron temperature studies using satellite observations and a theoretical model, *J. Geophys. Res.*, *101*, 15,323, 1996a.

Balan, N., K.-I. Oyama, G. J. Bailey, and T. Abe, Plasmasphere electron temperature profiles and the effects of photoelectron trapping and an equatorial high-altitude heat source, *J. Geophys. Res.*, *101*, 21,689, 1996b.

Balan, N., G. J. Bailey, M. A. Abdu, K.-I. Oyama, P. G. Richards, J. MacDougall, and I. S. Batista, Equatorial plasma fountain and its effects over three locations: Evidence for an additional layer, the F_3 layer, *J. Geophys. Res.*, *102*, 2047, 1997.

Banks, P. M., and A. F. Nagy, Concerning the influence of elastic scattering upon photoelectron transport and escape, *J. Geophys. Res.*, *75*, 1902, 1970.

Batista, I. S., T. de Medeiros, M. A. Abdu, and J. R. de Souza, Equatorial ionospheric vertical plasma drift model over the Brazilian region, *J. Geophys. Res.*, *101*, 10,887, 1996.

Bauer, S. J., and A. F. Nagy, Ionospheric direct measurement techniques, *Proc. IEEE*, *63*, 230, 1975.

Bilitza, D., Description of the mean behavior of ionospheric plasma temperature, *Adv. Space Res.*, *7*(6), 93, 1987.

Brace, L. H., and R. F. Theis, Global empirical models of ionospheric electron temperature in the upper *F* region and plasmasphere based on in situ measurements from the Atmosphere Explorer-C, ISIS-1 and ISIS-2 satellites, *J. Atmos. Terr. Phys.*, *43*, 1317, 1981.

Farley, D. T., Early incoherent scatter observations at Jicamarca, *J. Atmos. Terr. Phys.*, *53*, 665, 1991.

Fejer, B. G., *F* region plasma drifts over Arecibo: Solar cycle, seasonal, and magnetic activity effects, *J. Geophys. Res.*, *98*, 13,645, 1993.

Fejer, B. G., E. R. de Paula, S. A. Gonzales, and R. F. Woodman, Average vertical and zonal *F* region plasma drifts over Jicamarca, *J. Geophys. Res.*, *96*, 13,901, 1991.

Hanson, W. B., A. F. Nagy, and R. J. Moffett, OGO 6 measurements of supercooled plasma in the equatorial exosphere, *J. Geophys. Res.*, *78*, 751, 1973.

Hari, S. S., and B. V. Krishna Murthy, Equatorial nighttime *F* region zonal electric fields, *Ann. Geophys.*, *13*, 871, 1995.

Hedin, A. E., MSIS-86 thermospheric model, *J. Geophys. Res.*, *92*, 4649, 1987.

Hedin, A. E., and H. G. Mayr, Magnetic control of the near equatorial neutral thermosphere, *J. Geophys. Res.*, *78*, 1688, 1973.

Hedin, A. E., et al., Revised global model of thermosphere winds using satellite and ground-based observations, *J. Geophys. Res.*, *96*, 7657, 1991.

Kelley, M. C., Equatorial spread-*F*: Recent results and outstanding problems, *J. Atmos. Terr. Phys.*, *47*, 745, 1985.

Khazanov, G. V., and M. W. Liemohn, Nonsteady-state ionosphere-plasmasphere coupling of superthermal electrons, *J. Geophys. Res.*, *100*, 9669, 1995.

Khazanov, G. V., M. W. Liemohn, T. I. Gombosi, and A. F. Nagy, Nonsteady-state transport of superthermal electrons in the plasmasphere, *Geophys. Res. Lett.*, *20*, 2821, 1993.

Kohnlein, W., A model of the electron and ion temperatures in the ionosphere, *Planet. Space Sci.*, *34*, 609, 1986.

Moffett, R. J., The equatorial anomaly in the electron distribution of the terrestrial *F*-region, *Fundam. Cosmic Phys.*, *4*, 313, 1979.

Moffett, R. J., B. Jenkins, and G. J. Bailey, A modeling study of anisotropic ion temperatures generated in the *F* layer by subauroral ion drifts, *Ann. Geophys.*, *11*, 1051, 1993.

Namboothiri, S. P., N. Balan, and P. B. Rao, Vertical plasma drifts in the *F* region at the magnetic equator, *J. Geophys. Res.*, *94*, 12,055, 1989.

Newberry, I. T., R. H. Comfort, P. G. Richards, and C. R. Chappell, Thermal He^+ in the plasmasphere: Comparison of observations with numerical calculations, *J. Geophys. Res.*, *94*, 15,265, 1989.

Ossakow, S. L., Spread-*F* theories—A review, *J. Atmos. Terr. Phys.*, *43*, 437, 1981.

Oyama, K.-I., and K. Schlegel, Observations of electron temperature anisotropy in the ionosphere: A review, *Ann. Geophys.*, *6*, 389, 1988.

Oyama, K.-I., K. Schlegel, and S. Watanabe, Temperature structure of plasma bubbles in the low latitude ionosphere around 600 km altitude, *Planet. Space Sci.*, *36*, 553, 1988.

Oyama, K.-I., N. Balan, S. Watanabe, T. Takahashi, F. Isoda, G. J. Bailey, and H. Oya, Morning overshoot of Te enhanced by downward plasma drift in the equatorial topside ionosphere, *J. Geomagn. Geoelectr.*, *48*, 959, 1996.

Oyama, K.-I., M. A. Abdu, N. Balan, G. J. Bailey, S. Watanabe, T. Takahashi, E. R. de Paula, I. S. Batista, F. Isoda, and H. Oya, High electron temperature associated with the prereversal enhancement in the equatorial ionosphere, *J. Geophys. Res.*, *102*, 417, 1997.

Raghavarao, R., L. E. Wharton, N. W. Spencer, H. G. Mayr, and L. H. Brace, An equatorial temperature and wind anomaly, *Geophys. Res. Lett.*, *18*, 1193, 1991.

Rajaram, G., Structure of the equatorial *F*-region, topside and bottomside—A review, *J. Atmos. Terr. Phys.*, *39*, 1125, 1977.

Reddy, C. A., The equatorial electrojet: A review of ionospheric and geomagnetic effect, *J. Atmos. Terr. Phys.*, *43*, 557, 1981.

Richards, P. G., and D. G. Torr, Thermal coupling of conjugate ionospheres and the tilt of the Earth's magnetic field, *J. Geophys. Res.*, *91*, 9017, 1986.

Richards, P. G., and D. G. Torr, Ratios of photoelectron to EUV ionization rates for aeronomic studies, *J. Geophys. Res.*, *93*, 4060, 1988.

Richards, P. G., J. A. Fennelly, and D. G. Torr, EUVAC: A solar EUV flux model for aeronomic calculations, *J. Geophys. Res.*, *99*, 8981, 1994.

Rishbeth, H., T. E. VanZandt, and W. B. Hanson, Ion temperature troughs in the equatorial topside ionosphere, *Planet. Space Sci.*, *25*, 629, 1977.

Sastri, J. H., Equatorial anomaly in *F* region—A review, *Indian J. Radio Space Phys.*, *19*, 225, 1990.

Sayers, J., In situ probes for ionospheric investigations, *J. Atmos. Terr. Phys.*, *32*, 663, 1970.

Schunk, R. W., and A. F. Nagy, Electron temperatures in the *F* region of the ionosphere: Theory and observations, *Rev. Geophys.*, *16*, 355, 1978.

Stening R. J., Modeling the low-latitude *F* region, *J. Atmos. Terr. Phys.*, *54*, 1387, 1992.

Su, Y. Z., K.-I. Oyama, G. J. Bailey, T. Takahashi, and S. Watanabe, Comparison of satellite electron density and temperature measurements at low latitudes with a plasmasphere-ionosphere model, *J. Geophys. Res.*, *100*, 14,591, 1995.

Tobiska, W. K., Revised solar extreme ultraviolet flux model, *J. Atmos. Terr. Phys.*, *53*, 1005, 1991.

Walker, G. O., Longitudinal structure of the *F*-region equatorial anomaly—A review, *J. Atmos. Terr. Phys.*, *43*, 763, 1981.

Watanabe, S., and K.-I. Oyama, Effects of neutral wind on the electron temperature at a height of 600 km in the low latitude region, *Ann. Geophys.*, *14*, 290, 1996.

Watanabe, S., K.-I. Oyama, and M. A. Abdu, A computer simulation of electron and ion densities and temperature in the equatorial *F* region and comparison with Hinotori results, *J. Geophys. Res.*, *100*, 14,581, 1995.

M. A. Abdu, Instituto Nacional de Pesquisas Espaciais, Caixa Postal 515, 12201-970, São José dos Campos, São Paulo, Brazil. (e-mail: abdu@dae.inpe.br)

G. J. Bailey, School of Mathematics and Statistics, Applied Mathematics Section, University of Sheffield, Sheffield S3 7RH, England. (e-mail: g.bailey@sheffield.ac.uk)

N. Balan and S. Fukao, Radio Atmospheric Science Center, Kyoto University, Uji, Kyoto 611, Japan. (e-mail: balan@kurasc.kyoto-u.ac.jp; fukao@kurasc.kyoto-u.ac.jp)

K.-I. Oyama, Institute of Space and Astronautical Science, 3-1-1 Yoshinodai, Sagamihara, Kanagawa 229, Japan. (e-mail: oyama@bochan.ted.isas.ac.jp)

S. Watanabe, Department of Astronomy and Geophysics, Tohoku University, Aramaki, Aoba, Sendai, Japan. (e-mail: shw@stpp2.geophys.tohoku.ac.jp)

(Received August 23, 1996; revised December 23, 1996;
accepted January 2, 1997.)